

Theory of ac Space-Charge Polarization Effects in Photoconductors, Semiconductors, and Electrolytes

J. ROSS MACDONALD*

Chemistry Division, Argonne National Laboratory, Lemont, Illinois

(Received March 30, 1953)

A linear theory is developed of the ac behavior of solid or liquid materials containing charge carriers which can move freely within the material but cannot leave it through the electrodes. The theory applies for any degree of dissociation of neutral centers and recombination of positive and negative charge carriers, but these carriers are assumed to have been produced by dissociation from only one species of neutral center. The mobile carriers may be electrons, positive holes, positive ions, negative ions, positive ion vacancies, or negative ion vacancies. The general solution for the admittance of the material is obtained for an arbitrary ratio between the mobilities of positive and negative carriers, but, because of the complexity of the result, it is only discussed in detail in the present paper for the following special cases: (a) charge carriers of only one sign mobile, arbitrary recombination

time; (b) charge carriers of both signs mobile with the same mobility, arbitrary recombination time; and (c) charge carriers of both signs mobile with unequal mobilities and very short recombination time. In case (a), two dispersion regions may appear, with that at lower frequencies arising from recombination and the other from the finite mobility of the carriers. Both regions follow Debye dispersion curves accurately over a wide frequency range, making it possible to represent the electrical behavior of the material for any recombination time by means of a simple equivalent circuit containing only frequency-independent elements. In cases (b) and (c), only the motional dispersion region appears, and it again follows Debye curves. Finally, the results of the present theory are compared with those of other theories of ac space-charge effects in semiconductors and electrolytes.

I. INTRODUCTION

POLARIZATION effects arising from the motion of charge carriers under the influence of an electric field in materials with blocking electrodes have been extensively investigated in the past both experimentally and theoretically.¹ Jaffé has recently renewed interest in this subject with his treatment of ac polarization effects due to ionic motion in semiconductors² and in electrolytic solutions.³ In this paper, we derive expressions for ac polarization capacitance and conductance applying to any material which contains mobile charge carriers for which the electrodes are blocking. The treatment applies for any degree of dissociation and recombination and for any ratio between the mobilities of positive and negative charge carriers. The mobile carriers may be electrons, positive holes, positive ions (including donators), negative ions (including acceptors), or positive or negative ion vacancies.

The case considered here is considerably more general than those analyzed by Jaffé, and the solution obtained herein is less approximate than Jaffé's. In his treatment with Chang of electrolytes,³ he has assumed the presence of completely dissociated positive and negative ions of equal mobility, although it seems unlikely that the assumption of equal mobility can often be fulfilled in actuality. In his paper on the conductivity of semiconductors,² on the other hand, he discusses the equations governing charge carrier motion in a general way but derives results for space-charge capacitance and conductance applying only to the case where the com-

pletely dissociated charge carriers are electrons or positive holes of high mobility and positive ions and negative ions of low mobility, respectively.

The present work was undertaken because it was felt that previous treatments were insufficiently applicable to some physical situations which might be important in practice. The impurity centers in many semiconductors are not completely ionized at room or lower temperature, and the analysis of the response of these materials to applied fields must therefore take recombination into account. Further, many materials, such as photoconducting phosphors and *F*-centered alkali-halide crystals, contain neutral centers whose potential energy is so great that they can only be ionized in any appreciable number at room temperature by the absorption of light. Since tremendously large light intensities would be required to keep a large fraction of the neutral light-absorbing centers in such materials dissociated, only a small proportion of these centers would be ionized with the usual light intensities. Finally, at room temperatures, the mobilities of the ionized centers (positive or negative ions, positive or negative ion vacancies) in many materials are sufficiently small that their motion may be neglected except for applied frequencies considerably below the usual range of interest. The theory developed herein has been used to explain the photocapacitive effect⁴ in alkali-halide crystals in detail. This effect affords a good example for comparison of theory and experiment because the number of neutral *F* centers is easily varied by exposure to ultraviolet light or gamma-rays, and the number of dissociated centers conveniently controlled by means of the incident light intensity in the *F*-absorption band. The present theory applies, in addition, to electrolytes, but it has been necessary to postpone to a later paper a detailed discussion of the results of the theory for electrolytes and

* On leave from Armour Research Foundation of Illinois Institute of Technology. Now at Texas Instruments, 6000 Lemmon Avenue, Dallas 9, Texas.

¹ G. Jaffé, *Ann. Physik* **16**, 217, 249 (1933).

² G. Jaffé, *Phys. Rev.* **85**, 354 (1952).

³ H. Chang and G. Jaffé, *J. Chem. Phys.* **20**, 1071 (1952). References to the older literature are given in this paper and in reference 1.

⁴ J. R. Macdonald, *Phys. Rev.* **85**, 381 (1952); **90**, 364 (1953).

other materials containing both positive and negative carriers of unequal, nonzero mobilities and long or infinite recombination time.

In the following section, the applicable equations of the problem are solved on the basis of certain reasonable approximations. In Sec. III the resulting expressions for conductance and capacitance are plotted and tabulated *versus* frequency for the three cases (a) equal mobilities of the charge carriers, (b) zero recombination time and different mobilities, and (c) either positive or negative carriers immobile, any recombination time. Finally, in Sec. IV, the results of the analysis are compared, particularly in regard to frequency dependence, with those of several other space-charge polarization theories and with the Fuoss-Kirkwood theory of dielectric dispersion in materials having a distribution of relaxation times.⁵ In addition, the methods of analysis of experimental data allowing most simple comparison of theory and experiment are discussed.

II. SOLUTION OF THE EQUATIONS OF DETAILED BALANCE

Let N denote the initial concentration of immobile neutral centers before any dissociation takes place; p the concentration of positive charge carriers of mobility μ , diffusion coefficient D ; and n the concentration of negative carriers of mobility μ' and coefficient of diffusion D' .⁶ Assume that the two electrodes are at $x=0$ and $x=L$ and are blocking for both positive and negative carriers. Both n and p will, in general, be functions of x as well as time, both because of the motion of the charges and because of the presence of continuous dissociation and recombination throughout the layer. On dissociation, a neutral center produces a mobile negative carrier and a mobile positive carrier. The number of carriers produced per second at a position x will be proportional to the product of the concentration of neutral centers at x and a rate constant k_1 . This constant k_1 will depend on temperature and will also be directly proportional to light intensity if dissociation can be induced by absorption of light. It is assumed that in the case where the negative carriers are electrons, the electron concentration in the conduction band is sufficiently small that the influence of the Boltzmann factor for the conduction band levels may be neglected.

To simplify the treatment, the concentration of any extraneous traps for charge carriers will be taken vanishingly small and all carriers present will be assumed to have come from the N neutral centers. Under this assumption, the total number of negative carriers in the layer L must be equal to the total number of positive carriers. At any given time and position within the layer, p need not equal n , however. Finally, the initial distribution of neutral centers will be assumed to be uniform throughout the layer before any dissociation occurs. After some dissociation has taken place, the

concentration of neutral centers may be a function of x and time and will be denoted by n_c .

If recombination takes place, the number per cc of positive and negative carriers recombining to form neutral centers per sec will be given by k_2np , where k_2 is another rate constant which will not depend directly on light intensity and may depend on temperature less strongly than k_1 . The use of the term $k_2n(x, t)p(x, t)$ is an approximation since it specifies that the recombination rate is proportional to the concentration of positive centers and negative carriers present at the same position at the same time. In actuality, recombination can take place whenever a negative carrier approaches within a sphere of influence surrounding a positive carrier defined by specifying a capture probability distribution function. A treatment of diffusion taking the sphere of influence into account has been given by Chandrasekhar.⁷ This analysis might possibly be modified and incorporated into the present treatment, but it would add considerable complexity without a very large increase in accuracy. Therefore, the simple bimolecular k_2np term will be employed in the present work. It should also be mentioned that when holes and electrons are simultaneously present, their recombination may take place through the medium of traps.⁸ The k_2np recombination term will no longer be appropriate in this case for all carrier densities.

With these preliminaries, the equations of detailed balance including the effects of diffusion and motion under the influence of an applied electric field E may be written as^{2,9}

$$\partial p / \partial t = k_1 n_c - k_2 n p + D \partial^2 p / \partial x^2 - \mu \partial (pE) / \partial x, \quad (1)$$

$$\partial n / \partial t = k_1 n_c - k_2 n p + D' \partial^2 n / \partial x^2 + \mu' \partial (nE) / \partial x, \quad (2)$$

$$\partial n_c / \partial t = -k_1 n_c + k_2 n p, \quad (3)$$

where it has been assumed that the diffusion coefficient for the neutral centers is negligibly small.

In addition, we have specified that

$$\int_0^L p(x, t) dx = \int_0^L n(x, t) dx \quad (4)$$

must hold for all time. The charge densities must also satisfy the Poisson equation,

$$\partial E / \partial x = \beta (p - n), \quad (5)$$

where $\beta = 4\pi e / \epsilon$; ϵ is the dielectric constant of the material at the frequency considered;¹⁰ and e is the

⁷ S. Chandrasekhar, *Revs. Modern Phys.* **15**, 61 (1943).

⁸ W. Shockley and W. T. Read, Jr., *Phys. Rev.* **87**, 835 (1952).

⁹ W. Van Roosbroek, *Bell System Tech. J.* **29**, 560 (1950). Some further discussion of the equations is given in this reference.

¹⁰ Here ϵ includes the usual contributions of the lattice and bound charges and is thus the dielectric constant of the material in the absence of free charges. If there is dispersion in the ordinary dielectric response of the material in the frequency range considered, $\epsilon(f)$ will be complex for a given frequency f within this range. ϵ will, however, be taken as real in this paper.

⁵ J. R. Macdonald, *J. Chem. Phys.* **20**, 1107 (1952).

⁶ A glossary of principal symbols is given at the end of this paper.

charge of a carrier.¹¹ If the voltage between the electrodes is $V(t)$, we also require that

$$V(t) = \int_0^L E(x, t) dx. \quad (6)$$

Finally, since it has been assumed that both electrodes are blocking for both positive and negative carriers, no conduction current arising from the motion of either type of carrier can flow across the electrodes, and the pertinent boundary conditions are

$$\left. \begin{aligned} \mu p E - D \partial p / \partial x &= 0 \\ \mu' n E + D' \partial n / \partial x &= 0 \end{aligned} \right\} \text{at } x=0, L. \quad (7)$$

Equations (1) to (8) are the fundamental equations of the problem. They tacitly neglect the image force which acts on the carriers when they are near the electrodes. The neglect of this force is valid unless the thickness of polarization layers set up at the electrodes is less than about 10^{-6} cm. In practice, the layers are almost always thicker than this.

We shall now solve these equations for n , p , and E for a simple sinusoidal forcing voltage

$$V(t) = V_1 e^{i\omega t}. \quad (9)$$

Since the equations are nonlinear, the current through the medium will contain all harmonics of the forcing voltage, and accurate solutions for n , p , and E would show that they would all involve zero frequency (static) components together with the fundamental and all its overtones. By taking V_1 sufficiently small, the ratio of higher harmonic components to the fundamental component in n , p , and E may be made negligible, however. In a later paper on the photocapacitive effect, it will be shown experimentally that a value of V_1 so large that the distribution of n is extremely inhomogeneous still leads to only very small harmonic generation. It is therefore valid here to follow Jaffé² and assume that all harmonics above the fundamental may be neglected. Then, n , p , n_c , and E may all be written in the form

$$n(x, t) = n_0(x) + n_1(x) e^{i\omega t}. \quad (10)$$

The last approximation which we shall need to make to simplify the solution of the equations is the assumption that the static concentrations n_0 and p_0 are equal. Let their mutual value be c_0 . It then follows from Eqs. (1) to (10) that $E_0 = 0$ and that c_0 is homogeneous and frequency-independent. This assumption cannot be completely correct because it leads to expressions for $|n_1|$ and $|p_1|$ which may be larger than c_0 near the boundaries for large applied ac voltage. Physically, however, it is obvious that p_0 and n_0 must be equal to or greater than $|p_1|$ and $|n_1|$, respectively, at every

¹¹ We shall assume that each elementary carrier has a single electronic charge; the results of the theory are readily generalized to the cases of carriers of different charges and/or more than one electronic charge.

point in the material; otherwise, the over-all concentrations p and n would go negative during part of each cycle. Near the electrodes, then, p_0 and n_0 will actually be neither equal nor homogeneous. Since the polarization capacity and conductance are directly determined by n_1 , p_1 , and E_1 and only indirectly by the coupling of these quantities to n_0 , p_0 , and E_0 , it appears reasonable to assume that the ac capacitance and conductance will not be greatly affected by the neglect of the frequency and x dependence of the latter static quantities. This assumption has been verified by measurements on the photocapacitive effect, where it was found that ac capacitance and conductance are not appreciably affected by applying a dc bias field to the material many times greater than the small ac measuring field strength, even though such a bias must certainly alter the dependence of n_0 , p_0 , and E_0 on x greatly from the normal zero-bias condition.¹²

Since n_0 and p_0 are assumed equal and homogeneous, the static concentration of neutral centers n_{c0} will be simply $(N - c_0)$, which is also homogeneous. Using this value and $n_0 = p_0 = c_0$, we find, on substituting expressions of the form of (10) into the earlier equations,

$$i\omega p_1 = k_1 n_{c1} - k_2 (p_1 + n_1) c_0 + D d^2 p_1 / dx^2 - \mu c_0 dE_1 / dx, \quad (11)$$

$$i\omega n_1 = k_1 n_{c1} - k_2 (p_1 + n_1) c_0 + D' d^2 n_1 / dx^2 + \mu' c_0 dE_1 / dx, \quad (12)$$

$$0 = -k_1 (N - c_0) + k_2 c_0^2, \quad (13)$$

$$i\omega n_{c1} = -k_1 n_{c1} + k_2 (n_1 + p_1) c_0, \quad (14)$$

$$\int_0^L (n_1 - p_1) dx = 0, \quad (15)$$

$$dE_1 / dx = \beta (p_1 - n_1), \quad (16)$$

$$V_1 = \int_0^L E_1 dx, \quad (17)$$

$$\left. \begin{aligned} \mu c_0 E_1 - D d p_1 / dx &= 0 \\ \mu' c_0 E_1 + D' d n_1 / dx &= 0 \end{aligned} \right\} \text{at } x=0, L. \quad (18)$$

$$\left. \begin{aligned} \mu c_0 E_1 - D d p_1 / dx &= 0 \\ \mu' c_0 E_1 + D' d n_1 / dx &= 0 \end{aligned} \right\} \text{at } x=0, L. \quad (19)$$

Equation (13) may be solved for c_0 and yields

$$c_0 = [(k_1/2k_2)^2 + (k_1/k_2)N]^{\frac{1}{2}} - k_1/2k_2. \quad (20)$$

For the case of small dissociation, this reduces to

$$c_0 \cong [(k_1/k_2)N]^{\frac{1}{2}}, \quad (21)$$

whereas for complete dissociation c_0 is equal to N . These results are just the field-free equilibrium values which, according to our second approximation, are assumed

¹² The assumption that n_0 equals p_0 is restrictive of the class of physical situations to which the theory will apply, especially for semiconductors where it excludes all but completely intrinsic or completely impurity types. When n_0 and p_0 are unequal but may, to an adequate approximation, be assumed homogeneous, it is found that the general form of the present solution remains unchanged. Therefore, this solution is a useful first step in the treatment of more complex physical situations.

to apply to the present case as well. Solving Eq. (14) for n_{c1} , one finds

$$n_{c1} = \lambda(\phi_1 + n_1), \quad (22)$$

where

$$\lambda \equiv \frac{1}{[(k_1/k_2c_0) + i\nu_r]}, \quad (23)$$

and ν_r is a dimensionless frequency variable given by

$$\nu_r \equiv \omega/k_2c_0 \equiv \omega\tau_r. \quad (24)$$

The quantity k_1/k_2c_0 appearing in (23) is just c_0/N in the case of small dissociation and thus is then small compared to unity. The time constant τ_r in (24) is the mean lifetime of an excess carrier for volume recombination. The recombination constant k_2 is usually less than 10^{-8} cm³/sec. The dimensionless, frequency-dependent quantity λ is, from (22), the ratio of the fundamental frequency component of charge bound in the neutral centers to the fundamental component of free charge arising from such centers.

In order to solve for the x dependence of n_1 and ϕ_1 , one can now substitute Eqs. (16) and (22) into (11) and (12). After collecting² terms, the³ results may be written

$$d^2\phi_1/dx^2 = a_{11}\phi_1 + a_{12}n_1, \quad (25)$$

$$d^2n_1/dx^2 = a_{21}\phi_1 + a_{22}n_1, \quad (26)$$

where

$$a_{11} = 2(M/L)^2[1 + i\sigma(1 + \lambda)\nu], \quad (27)$$

$$a_{12} = 2(M/L)^2[-1 + i\lambda\sigma\nu], \quad (28)$$

$$a_{21} = 2(M/L)^2[-1 + i\lambda\nu], \quad (29)$$

$$a_{22} = 2(M/L)^2[1 + i(1 + \lambda)\nu], \quad (30)$$

and

$$(M/L)^2 = \mu'c_0\beta/2D' = 2\pi e c_0\mu'/\epsilon D' = 2\pi e^2c_0/\epsilon kT, \quad (31)$$

$$\sigma = \mu'/\mu = D'/D, \quad (32)$$

$$\nu = \omega/\mu'c_0\beta = \epsilon f/2\mu'ec_0. \quad (33)$$

The Einstein relation¹³ $\mu/D = \mu'/D' = e/kT$ has been used in (31) and (32). ν is another dimensionless frequency variable connected with the motion of the charge carriers.

The characteristic equation associated with Eqs. (25) and (26) is easily solved. After simplification, its roots are

$$\begin{aligned} [\rho^\pm]^2 = & 2\left(\frac{M}{L}\right)^2 \left[1 + i(1 + \lambda)\left(\frac{1 + \sigma}{2}\right)\nu \right. \\ & \pm \left\{ 1 - \left[\lambda\left(\frac{\sigma + 1}{2}\right)\nu \right]^2 - (1 + 2\lambda)\left[\left(\frac{\sigma - 1}{2}\right)\nu \right]^2 \right. \\ & \left. \left. - i\lambda(1 + \sigma)\nu \right\}^{\frac{1}{2}} \right]. \quad (34) \end{aligned}$$

¹³ A. Einstein, Ann. Physik 17, 549 (1905).

There are thus four roots, and n_1 and ϕ_1 will be given by the sum of four terms each of the form $\exp[\rho x]$. Considerable simplification is produced, however, when the symmetry of the problem is taken into account. From symmetry considerations it is obvious that n_1 and ϕ_1 must be odd functions of x about the center of the slab at $L/2$. They may therefore be written as

$$n_1 = A^+ \sinh[\rho^+(x - L/2)] + A^- \sinh[\rho^-(x - L/2)], \quad (35)$$

$$\phi_1 = B^+ \sinh[\rho^+(x - L/2)] + B^- \sinh[\rho^-(x - L/2)]. \quad (36)$$

The four A 's and B 's may now be determined through the use of Eqs. (16), (17), (18), (19), (25), and (26). It is easy to see that these six equations do not overdetermine the four unknowns. The results are

$$A^+/B^+ \equiv \gamma^+ = a_{21}/[(\rho^+)^2 - a_{22}] = [(\rho^+)^2 - a_{11}]/a_{12}, \quad (37)$$

$$A^-/B^- \equiv \gamma^- = a_{21}/[(\rho^-)^2 - a_{22}] = [(\rho^-)^2 - a_{11}]/a_{12}, \quad (38)$$

$$-\frac{A^+}{A^-} \equiv \chi_A = \frac{\gamma^+\rho^-(1 + \gamma^-) \cosh \eta^-}{\gamma^-\rho^+(1 + \gamma^+) \cosh \eta^+}, \quad (39)$$

and

$$\begin{aligned} V_1 = & \frac{2D'A^-}{\mu'c_0} \left[\chi_A \left\{ \left(\frac{1}{\gamma^+} - 1\right) \left(\frac{L\rho^+}{\sqrt{2}M}\right)^{-2} + 1 \right\} \eta^+ \cosh \eta^+ \right. \\ & - \left\{ \left(\frac{1}{\gamma^-} - 1\right) \left(\frac{L\rho^-}{\sqrt{2}M}\right)^{-2} + 1 \right\} \eta^- \cosh \eta^- \\ & - \chi_A \left(\frac{1}{\gamma^+} - 1\right) \left(\frac{L\rho^+}{\sqrt{2}M}\right)^{-2} \sinh \eta^+ \\ & \left. + \left(\frac{1}{\gamma^-} - 1\right) \left(\frac{L\rho^-}{\sqrt{2}M}\right)^{-2} \sinh \eta^- \right], \quad (40) \end{aligned}$$

where

$$\eta^\pm = L\rho^\pm/2. \quad (41)$$

These dimensionless quantities η^\pm largely determine the frequency dependence of the admittance of the material between the electrodes.

Now, the current entering and leaving the layer of thickness L can be computed and from it the complex admittance of the whole layer considered as a lumped circuit element. The current density within the layer will be given by the sum of a displacement term and two convection terms arising from the motion of positive and negative charges. It is

$$j_1(x) = \frac{\epsilon}{4\pi} \frac{\partial E}{\partial t} + e \left[\mu c_0 E_1 - D \frac{d\phi_1}{dx} + \mu' c_0 E_1 + D' \frac{dn_1}{dx} \right]. \quad (42)$$

The total current density flowing into the layer can be obtained by taking a space average of $j_1(x)$ over the

whole layer.¹⁴ One obtains

$$J_1 \equiv Y_1 V_1 = \frac{i\omega\epsilon V_1}{4\pi L} + \frac{e}{L} [(\mu + \mu')c_0 V_1 - D\{p_1(L) - p_1(0)\} + D'\{n_1(L) - n_1(0)\}]. \quad (43)$$

The admittance/cm², Y_1 , is made up of a term arising

$$Y_P = \frac{e(\mu + \mu')c_0}{L} + \frac{ec_0\mu'}{L} \left[\frac{\chi_A \left(1 - \frac{1}{\sigma\gamma^+}\right) \sinh\eta^+ - \left(1 - \frac{1}{\sigma\gamma^-}\right) \sinh\eta^-}{\chi_A \left(1 - \frac{1}{\gamma^+}\right) \left(\frac{L\rho^+}{\sqrt{2}M}\right)^{-2} (\eta^+ \cosh\eta^+ - \sinh\eta^+) - \chi_A \eta^+ \cosh\eta^+ - \left(1 - \frac{1}{\gamma^-}\right) \left(\frac{L\rho^-}{\sqrt{2}M}\right)^{-2} (\eta^- \cosh\eta^- - \sinh\eta^-) + \eta^- \cosh\eta^-} \right] = G_P + i\omega C_P, \quad (44)$$

and

$$C_g = \epsilon/4\pi L. \quad (45)$$

This is a very complicated, complex formula for C_P and G_P , and in the present paper we shall only consider the reductions of this formula in various limiting cases, reserving a discussion of the general formula (44) for a later paper.

Before considering the reductions of (44), it appears to be of interest to compare the present result and mode of attack with that of Chang and Jaffé in their paper on polarization effects in electrolytic solutions.³ The case considered by them was that of complete dissociation with no recombination, and the positive and negative carriers were assumed to be of equal mobility. Rather than determine E_1 from the equations of the problem in such a manner that Poisson's equation is satisfied, as is done in the present work, they used an expression for E_1 determined from an earlier solution for the dc case.¹ Their expression does not satisfy Poisson's equation, nor is it complex as the true ac field must be. Further, the field inhomogeneity does not depend on frequency as physical reasoning shows it must. In an effort to remove some of these inconsistencies, Chang and Jaffé applied their solution to a "polarization layer" of thickness l ($\leq L$) only. They then split this layer in half, put the halves at the electrodes, and assumed that there were no polarization effects in a bulk layer located between the $l/2$ -thick layers. By satisfying boundary conditions at the junction of polarization and bulk layers, they were able to determine an approximate dependence of l , and thus of field inhomogeneity, on frequency. These difficulties are automatically avoided in the present treatment, which is, in addition, more general. Here, the solution applies to the entire slab of

¹⁴ It is worth noting that since the convection current is zero at the boundaries, the total current J_1 entering the layer must be purely displacement current. Thus J_1 may alternatively be derived from $J_1 = (\epsilon/4\pi)(\partial E/\partial t)_{z=0} = (i\omega\epsilon/4\pi)E_1(0)$. The lack of a negative sign in this equation arises from our choice of the sign of V_1 or E_1 in Eqs. (6) and (9).

from the normal capacitance/cm², C_g , of the layer in the absence of macroscopic charge motion and terms coming from the space-charge parallel capacitance/cm² and conductance/cm², C_P and G_P , respectively. Let Y_P be the admittance/cm² due to space-charge effects alone. If we now substitute the preceding expressions for n_1 and p_1 in (43) using (37) to (40), we find

thickness L , and there is never (except at infinite frequency) any bulk layer in the middle of the slab where polarization effects are absolutely zero, although they are usually negligibly small near the center of the slab. There is thus no uniquely defined polarization layer, although the inhomogeneity of n and E increases rapidly near the boundaries.

Now let us consider the reduction of (44) for various limiting cases. It will prove convenient to introduce another dimensionless frequency variable ν^* given by

$$\nu^* \equiv \omega C_g / G_\infty = \omega\epsilon / 4\pi\sigma_\infty \equiv \omega\tau_D, \quad (46)$$

where G_∞ is the limiting value of G_P at very high frequencies and will, in all cases, be found to be the normal ohmic conductance/cm² of the slab which would obtain at all frequencies were the electrodes not blocking. Similarly, $\sigma_\infty \equiv LG_\infty$ is the limiting conductivity of the material. Thus, the time constant τ_D is the ordinary dielectric relaxation time for conductivity σ_∞ . It is too short to be measured electrically for metals and some highly conductive semiconductors, but corresponds to measurable frequencies for less conductive semiconductors, and for photoconductors and high resistivity electrolytes. For example, it is of the order of a microsecond for distilled water. In order to deal with a single frequency variable, we shall also define the ratio of recombination time to dielectric relaxation time ξ as

$$\xi = \nu_r / \nu^* = \tau_r / \tau_D = 4\pi\sigma_\infty / \epsilon k_2 c_0, \quad (47)$$

and use this relation to express ν_r in terms of ν^* . Since σ_∞ is proportional to c_0 , ξ is independent of carrier concentration. ξ will be infinite in the case of zero recombination (complete dissociation) and very small for rapid recombination.

We shall first consider the reduction of (44) in the limiting case of negative carriers alone mobile. Then $\mu = 0$ and $\sigma = \infty$. Let

$$\delta = \lambda / (1 + \lambda) = [1 + k_1 / k_2 c_0 + i\xi\nu^*]^{-1}. \quad (48)$$

From the definition of λ [Eq. (22)], δ is thus

$n_{c1}/(n_{c1}+p_1+n_1)$, i.e., the ratio of the fundamental frequency component of charge bound in neutral centers to the fundamental component of total charge, free and bound. Expansion of (34) gives

$$[\rho^+]^2 = \infty, \quad (49)$$

$$[\rho^-]^2 = 2(M/L)^2(1+\delta)(1+i\nu^*), \quad (50)$$

where we have used the expression for G_∞ , below, to convert ν to ν^* . In this particular limiting case they are identical. Thus

$$\eta^- = M[\frac{1}{2}(1+\delta)(1+i\nu^*)]^{\frac{1}{2}}. \quad (51)$$

For complete dissociation $\delta=0$, whereas for small dissociation, the k_1/k_2c_0 term in δ may be neglected compared to unity, and one finds

$$\eta^- = M[(1+i\xi\nu^*/2)(1+i\nu^*)/(1+i\xi\nu^*)]^{\frac{1}{2}}. \quad (52)$$

For arbitrary dissociation the expressions for C_P and G_P resulting from (44) are

$$C_P = \frac{C_0}{\eta_0^- \coth\eta_0^- - 1} \operatorname{Re} \left[\frac{\eta^- - \tanh\eta^-}{\tanh\eta^- + i\nu\eta^-} \right], \quad (53)$$

and

$$G_P = -\nu G_\infty \operatorname{Im} \left[\frac{\eta^- - \tanh\eta^-}{\tanh\eta^- + i\nu\eta^-} \right], \quad (54)$$

where

$$C_0 = (\eta_0^- \coth\eta_0^- - 1)C_g, \quad (55)$$

$$G_\infty = e\mu'c_0/L, \quad (56)$$

and η^- is given by (51), C_g by (45). η_0^- is the value of η^- when $\nu^*=0$. It is equal to M for small dissociation. C_0 is the zero-frequency limit of C_P . It should be mentioned that exactly the same expressions for C_P and G_P are obtained in the case of only positive carriers mobile with mobility μ' instead of μ .

The quantity M is of especial interest. In the present limiting case, M may be written

$$M = L/(2D'\tau_D)^{\frac{1}{2}} \equiv L/L_D. \quad (57)$$

M is thus the number of rms Debye lengths L_D contained in the thickness L between electrodes.¹⁵ Further, the distance from the electrodes over which the concentrations n_1 and p_1 drop by a factor of e^{-1} is approximately $L/2\operatorname{Re}(\eta^-)$ as long as this is much less than L . For zero frequency and small dissociation, this distance is $L_D/2$. At room temperature, the rms Debye length for a material of dielectric constant 10 and charge density $c_0=10^{14}/\text{cm}^3$ is 5.3×10^{-5} cm.

At zero frequency, $G_P=0$. Let us define

$$r = \eta_0^- \coth\eta_0^-; \quad (58)$$

¹⁵ The Debye length may be defined analogously to the recombination diffusion length $(D'\tau_r)^{\frac{1}{2}}$ as $(D'\tau_D)^{\frac{1}{2}}$. It is the average distance an excess carrier must travel to establish space-charge neutrality. The rms Debye length is $(2D'\tau_D)^{\frac{1}{2}}$. In the present case, the Debye length may be written as $[\epsilon kT/4\pi e^2 c_0]^{\frac{1}{2}}$ by using the Einstein relation. When there are many species of carriers of different mobilities and valencies z_i , the Debye length is $[\epsilon kT/4\pi e^2 \sum_i n_i z_i^2]^{\frac{1}{2}}$. In theories of electrolytes, it is called the thickness of the ionic atmosphere.

then $C_0 = (r-1)C_g$. Since C_g appears in parallel with C_P , r is the ratio of the measured parallel capacitance including space-charge polarization effects to that without such effects, in the limit of low frequencies. If this ratio can be conveniently measured directly, η_0^- may be immediately determined. In the interesting case of small dissociation, M is thus obtained and from it c_0 if ϵ is known. For r values greater than 3, η_0^- is closely equal to r , whereas for $r \leq 1.005$, η_0^- may be found from the limiting formula $\eta_0^- = [3(r-1)]^{\frac{1}{2}}$. In the intermediate region, the relation between η_0^- and r has been determined graphically and is presented in Table I. It is of particular interest to note that within the accuracy of the present approximation, the zero-frequency capacitance C_0 is independent of slab thickness L provided $r \gg 1$. In this case,

$$C_0 \cong \eta_0^- C_g = \left[\left(\frac{1+k_1/2k_2c_0}{1+k_1/k_2c_0} \right) \frac{e\mu'c_0}{8\pi D'} \right]^{\frac{1}{2}}. \quad (59)$$

Since C_g is inversely proportional to L , r may be made as large as desired by increasing L . For small dissoci-

TABLE I. The dependence of the dimensionless constant η_0^- on $r = \eta_0^- \coth\eta_0^- = (C_0 + C_g)/C_g$.

r	η_0^-	r	η_0^-
4	4	1.3	0.972
3	2.985	1.2	0.791
2.5	2.47	1.1	0.557
2	1.92	1.05	0.388
1.8	1.68	1.02	0.244
1.6	1.42	1.01	0.174
1.5	1.29	1.005	0.1225
1.4	1.14	1.002	0.0774

ation and rapid recombination

$$C_0 \cong MC_g = [e\mu'c_0/8\pi D']^{\frac{1}{2}} = \epsilon/4\pi L_D, \quad (60)$$

whereas for complete dissociation ($k_2=0$),

$$C_0 \cong MC_g/\sqrt{2} = [e\mu'c_0/16\pi D']^{\frac{1}{2}} = \epsilon/4\pi\sqrt{2}L_D. \quad (61)$$

In the two above cases, the zero-frequency space-charge capacitance/cm² is formed from the geometrical capacitance/cm² by using the rms Debye length (or $\sqrt{2}L_D$) in place of the normal electrode separation L .

All the foregoing expressions for C_0 , the low frequency limiting capacitance/cm², apply also to the zero frequency or dc case. The expressions for C_0 are, in fact, somewhat more exact than other quantities such as C_P appearing in the ac theory because the neglect of higher harmonics is not an approximation in the dc case as it is for finite frequencies.

Another case of interest is that of equal mobilities. Then $\sigma=1$, and we obtain

$$\eta^+ = M[1+i\nu/2]^{\frac{1}{2}} = M[1+i\nu^*]^{\frac{1}{2}}, \quad (62)$$

$$G_\infty = 2\mu'ec_0/L, \quad (63)$$

$$C_0 = (M \coth M - 1)C_g, \quad (64)$$

$$C_0 \cong MC_g = [\epsilon e c_0 \mu' / 8\pi D']^{\frac{1}{2}} = \epsilon/4\pi\sqrt{2}L_D, \quad (65)$$

where (65) holds only for $M \gg 1$. Note that the rms Debye length in this equation is $1/\sqrt{2}$ less than that appearing in (60) and (61) because here both positive and negative carriers are mobile. The expressions for C_P and G_P obtained for this case are exactly the same as those above but with η^+ replacing η^- and M replacing η_0^- . Further, the dependence on ν^* is also the same as the previous case for $\delta=1$ (zero recombination time). Since ξ does not appear in the equations of the present case, recombination has no effect. Note that Eqs. (64) and (55) give the same result for C_0 , in the case of rapid recombination and small dissociation, even though in one instance both types of carriers are mobile, in the other only carriers of one sign.

It is of interest to compare our results for G_∞ and C_0 given by (63) and (64) with the results of Chang and Jaffé³ for the same case of equal mobilities. Agreement is obtained for G_∞ , but Chang and Jaffé³ find the expression (65) for C_0 . This is approximately correct when $M \gg 1$ but is a very poor approximation to the more correct result (64) when $M < 1.5$. Since Chang and Jaffé applied their results to the interpretation of experiments on electrolytes for which $M \gg 1$, the approximate result was adequate for their purposes. In a later paper on the photocapacitive effect, we shall find experimentally that M may sometimes be less than unity, and the more correct result must be used.

Finally, let us consider the case of zero recombination time and unequal mobilities. In this case λ and k_2 are infinite and ξ is zero. We find

$$\eta^- = M \left[1 + i \left(\frac{\sigma}{1 + \sigma} \right) \nu \right]^{\frac{1}{2}} = M [1 + i\nu^*]^{\frac{1}{2}}. \quad (66)$$

Again, the same expressions are obtained for C_P , G_P , and C_0 as in the previous case. The expression for G_∞ now becomes

$$G_\infty = ec_0(\mu + \mu')/L, \quad (67)$$

however, as one would expect. For the results obtained in this case to apply, the recombination time does not, of course, have to be zero but only short compared to the dielectric relaxation time of the moving charge carriers.

In the three limiting cases which we have considered, we have found that the shape of the curves is the same and that the cases differ only in values of C_0 , G_∞ , and ν .¹⁶ Because of the correspondence between the different limiting cases, we may restrict attention to one of these cases only. We shall consider curve shape in detail only for the first case, that of mobile negative carriers, since it is this case which applies most closely to the photocapacitive effect and to many space-charge effects in solids. The results will include the effect of different

¹⁶ Since $\nu^* = \nu$ in the case of charges of only one sign mobile, for the sake of simplicity we shall use ν rather than ν^* in the succeeding work.

recombination rates and will apply¹⁶ both to small dissociation and to complete dissociation.

Before considering C_P and G_P curve shape in detail, it is of interest to give the expressions for E_1 , n_1 , and ϕ_1 in the case $\sigma = \infty$.¹⁶ The results are

$$\frac{E_1}{(V_1/L)} = \eta^- \left[\frac{\{\cosh\eta^-(1-2x/L)\}/\{\cosh\eta^-\} + i\nu}{\tanh\eta^- + i\nu\eta^-} \right], \quad (68)$$

$$\frac{n_1}{c_0} = \frac{V_1}{2} \frac{\mu'}{D'} \left[\frac{(1+i\nu) \sinh\eta^-(1-2x/L)}{\sinh\eta^- + i\nu\eta^- \cosh\eta^-} \right], \quad (69)$$

$$\phi_1 = -\delta n_1, \quad (70)$$

where η^- is given by (51) and δ by (48). These expressions show clearly how the inhomogeneity of n_1 and E_1 depends on x . For large M and small ν , the inhomogeneity of E_1 can be exceedingly large near the electrodes. The inhomogeneity of n , the total concentration of negative carriers, will not be appreciable, however, unless V_1 is large enough that $|n_1|$ is approximately equal to c_0 .

III. RESULTS OF THE THEORY IN THE CASE OF CHARGE CARRIERS OF ONLY ONE SIGN MOBILE

We shall now investigate the dependence of the normalized quantities C_P/C_0 and G_P/G_∞ on frequency for various values of ξ and M for the case of small dissociation. The results will also hold for the case of complete dissociation. However, there may be a region of incomplete but large dissociation where the neglect, compared to unity, of the k_1/k_2c_0 term in δ may not be permissible. Since this situation will occur only in the physically unlikely case of fast recombination and large dissociation, this term will be omitted in the following work. Since the expressions for the frequency dependence of C_P/C_0 and G_P/G_∞ are complicated, complex functions, an IBM card programmed calculator has been employed to compute this dependence for selected values of M and ξ .¹⁷

The results of many calculations show that the dispersion curve shapes depend critically upon the ratio ξ/M . When ξ/M is less than about 0.1, the curves are little altered from their shape for $\xi=0$. On the other hand, when ξ/M is greater than about 30, a double dispersion phenomenon appears. In the intermediate region, the shoulders of the curves are rounded compared with the $\xi=0$ curves.

We shall first consider the case of zero recombination time, corresponding to $\xi=0$. When M is greater than about 10, it is found that the C_P/C_0 and G_P/G_∞ curves may be approximated over a wide frequency range by

¹⁷ Material supplementary to this article has been deposited as Document number 4052 with the ADI Auxiliary Publications Project, Photoduplication Service, Library of Congress, Washington 25, D. C. A copy may be secured by citing the Document number and by remitting \$1.25 for photoprints, or \$1.25 for 35-mm microfilm. Advance payment is required. Make checks or money orders payable to: Chief, Photoduplication Service, Library of Congress.

simple Debye curves involving a single relaxation time, τ_m . The larger the value of M , the wider the range over which the approximation is valid.¹⁹ Some implications of this result have already been discussed.²⁰ The correspondence of the space-charge dispersion curves to Debye curves is best demonstrated by converting the parallel quantities C_P/C_0 and G_P/G_∞ to their equivalent series circuit values C_S/C_0 and G_S/G_∞ . If C_P/C_0 and G_P/G_∞ satisfy Debye curves for all frequencies, the series values, similarly normalized, will be unity for all frequencies. Therefore, any deviations of C_S/C_0 and G_S/G_∞ from unity will be a measure of the lack of agreement of C_P/C_0 and G_P/G_∞ with Debye curves. Conversion to series values shows that for frequencies corresponding to $\omega\tau_m \lesssim 5r$, C_S/C_0 is accurately unity but drops off toward zero for higher frequencies. Thus, the larger the value of M , the wider the range over which C_S is a constant. Similarly, G_S/G_∞ is found to be unity for very high frequencies but drops to a low-frequency limiting value G_0/G_∞ as the frequency decreases. This limiting value is

$$\frac{G_0}{G_\infty} = \frac{(M \coth M - 1)^2}{(3/2)M \coth M (M \coth M - 1) - M^2/2}, \quad (71)$$

and approaches unity as M increases.

Physically, the reason for the drop in C_S at high frequencies is associated with the finite mobility of the free charges. For small M , the space charge layers at the electrodes are relatively thick, and at high frequencies insufficient time is available for the layers to be completely established during a half cycle. Therefore, C_S begins to decrease as the frequency increases. The larger the value of M , however, the thinner the boundary layers and the quicker they can be established. It should be noted that although C_S eventually approaches zero for any value of M , its reactance nevertheless also approaches zero in the limit.

As a practical matter, it is probably impossible in general to determine C_P accurately for frequencies above which it has decreased to 0.1 or 0.01 of C_0 , since C_P is determined experimentally from the difference between the measured value and C_0 . Thus, in Table II the values of C_S/C_0 and G_S/G_∞ are given for various M values at the frequencies for which $C_P/C_0 = 0.1$ and 0.01. The corresponding values of C_P/C_0 at these frequencies are also given. For M equal to or greater than 100, the deviations from unity are small for both C_P/C_0 values. For the less stringent condition $C_P/C_0 = 0.1$, the deviations are small even for $M = 1$. The final column gives G_0/G_∞ for the various M values.

The motional relaxation time τ_m is readily determined from the dissipation factor D_m , arising from space-charge effects when this factor is expressed in terms of

series quantities. We obtain

$$\tau_m = D_m/\omega = R_S C_S = C_0/G_\infty = (r-1)\nu/\omega = (r-1)\tau_D. \quad (72)$$

τ_m is thus just the time constant of C_0 in series with G_∞ and is therefore the capacitive relaxation time associated with the space-charge layers at the electrodes. In contradistinction to τ_D it involves the separation between electrodes L . For large M , it is approximately

$$\tau_m = \frac{L}{\mu} \left[\frac{\epsilon}{8\pi c_0 kT} \right]^{\frac{1}{2}}. \quad (73)$$

For comparison of curves corresponding to different M values, it will be convenient to introduce another dimensionless frequency variable given by

$$\nu_m = \omega\tau_m = (r-1)\nu. \quad (74)$$

We shall actually plot C_P/C_0 and G_P/G_∞ curves *versus* $\sqrt{\nu_m}$ instead of ν_m both in order to reduce the number of decades necessary and to correspond with the work of Chang and Jaffé.³ It is found that curve shape does not depend very strongly on the value of M . Figure 1 is a doubly logarithmic plot of C_P/C_0 and G_P/G_∞ *versus* $\sqrt{\nu_m}$ for $M = 0.1$ and 100. In addition, $(1 - C_P/C_0)$ and

TABLE II. Dependence of C_P/C_0 , C_S/C_0 , and G_S/G_∞ upon M for $C_P/C_0 = 0.1$ and 0.01, and dependence of G_0/G_∞ on M .

M	$C_P/C_0 \approx 0.1$			$C_P/C_0 \approx 0.01$			$\nu = 0$ G_0/G_∞
	C_P/C_0	C_S/C_0	G_S/G_∞	C_P/C_0	C_S/C_0	G_S/G_∞	
1	0.3167	0.9764	0.8431	$3.092 \cdot 10^{-2}$	0.7583	0.8703	0.8408
10	$1.212 \cdot 10^{-2}$	0.9203	0.9568	$1.120 \cdot 10^{-3}$	0.6530	0.9698	0.9529
10^2	$1.021 \cdot 10^{-3}$	0.9886	0.9951	$1.110 \cdot 10^{-4}$	0.9106	0.9954	0.9950
10^4	$1.000 \cdot 10^{-5}$	1.000	1.000	$1.001 \cdot 10^{-6}$	0.9992	1.000	0.9999

$(1 - G_P/G_\infty)$ are included to show the details of the curves near saturation. The G_P/G_∞ and $(1 - G_P/G_\infty)$ curves are displaced to the right by one decade in order to show all curves clearly in one figure. For $M = 100$, the C_P/C_0 curve is an excellent Debye curve over the entire range shown. Thus, the deviation of the C_P/C_0 curve from the Debye values for $M = 0.1$ can readily be seen. The deviation is surprisingly small. On the other hand, the G_P/G_∞ curve for $M = 100$ is only well approximated by a Debye curve for $\sqrt{\nu_m}$ less than about 3, the point where the $(1 - G_P/G_\infty)$ line begins to curve. Similarly, for $M = 0.1$, agreement is good only for $\sqrt{\nu_m}$ less than unity. In the case of the G_P/G_∞ curve for $M = 100$, the departure from Debye values above $\sqrt{\nu_m} = 3$ is of no practical consequence since G_P/G_∞ is within about one percent of saturation at $\sqrt{\nu_m} = 3$. The dependence of C_P/C_0 and G_P/G_∞ on $\sqrt{\nu}$ for several M values is presented in Table III.

The crossover point, at which $C_P/C_0 = G_P/G_\infty$, should occur for Debye curves at $\nu_m = 1$. In Table IV, the values of $\sqrt{\nu_m}$ at crossover are presented for various M values with $\xi = 0$ and 100, and also for different ξ values with $M = 10$. It will be seen that the deviations from unity are not very great for any of the values.

¹⁸ This result may also be found by expanding the rigorous expressions for C_P and G_P . Because of the complexity of the resulting formulas, their correspondence to Debye curves is, however, better demonstrated by graphical comparison.

¹⁹ J. R. Macdonald, Phys. Rev. **91**, 412 (1953).

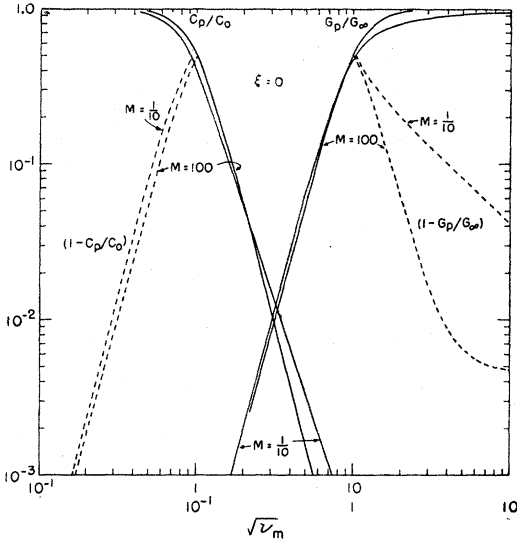


FIG. 1. Doubly logarithmic plot of C_P/C_0 and G_P/G_∞ versus $\sqrt{\nu_m}$ for $\xi=0$ and $M=0.1$ and 100 , solid lines. The dotted lines are $(1-C_P/C_0)$ and $(1-G_P/G_\infty)$. These curves apply only for zero recombination time. Note that G_P/G_∞ and $(1-G_P/G_\infty)$ curves are displaced one decade to the right for clarity.

The value of G_P/G_∞ and C_P/C_0 at crossover should be one-half. A decrease below this value sets in as M becomes small; however, this decrease is not usually important.

Although the dispersion curve shape is only slightly

dependent on M for $\xi=0$, this is no longer the case when ξ/M is large. Figure 2 is a doubly logarithmic plot of C_P/C_0 and G_P/G_∞ versus $\sqrt{\nu_m}$ for $\xi=100$ and $M=1$ and 100 . For $M=100$ the principal difference from the corresponding $\xi=0$ curves is a rounding of the shoulders.⁴ But for $M=1$ ($\xi/M=100$) a definite plateau appears in both the C_P/C_0 and G_P/G_∞ curves. The curves are thus made up of two dispersion regions, the lower frequency one arising from recombination, the higher from the motion of the charge carriers. This behavior is even more clearly demonstrated in Figs. 3 and 4 for $M=10$ and various values of ξ . In these curves the abscissa is $\sqrt{\nu}$ rather than $\sqrt{\nu_m}$. It will be noted that in Fig. 3 the shape of the lower-frequency dispersion curve is essentially independent of ξ for large ξ and that an increase in ξ merely displaces the two dispersion regions by lengthening the plateau. If the lower frequency dispersion region is treated separately, it is found that the dispersion curves arising from recombination alone are also well approximated by Debye curves over a wide frequency range if M is not too small. The two regions of dispersion may be separated by letting μ' go to infinity. Then ν goes to zero and $\xi\nu$ to ν_r . Making these substitutions in equations (52), (53), and (54), the expressions for C_P/C_0 and G_P/G_∞ pertaining to recombination alone may be obtained. Their dependence on $\sqrt{\nu_r}$ is presented in Table V. C_P/C_0 reaches a limiting value at high frequencies which will be denoted by C_∞/C_0 (the plateau in Fig. 3).

TABLE III. The dependence of C_P/C_0 and G_P/G_∞ on $\sqrt{\nu}$ for $M=0.1, 1$, and 100 , and $\xi=0$.

$\sqrt{\nu}$	$M=0.1$		$M=1$		$M=100$	
	C_P/C_0	G_P/G_∞	C_P/C_0	G_P/G_∞	C_P/C_0	G_P/G_∞
0.0100					0.9999	$9.849 \cdot 10^{-5}$
0.03162					0.9901	$9.753 \cdot 10^{-3}$
0.04217					0.9696	$3.020 \cdot 10^{-2}$
0.05623					0.9099	$8.963 \cdot 10^{-2}$
0.07499			1.000	$3.685 \cdot 10^{-6}$	0.7616	0.2372
0.1000			1.000	$1.165 \cdot 10^{-6}$	0.5025	0.4950
0.1334			1.000	$3.685 \cdot 10^{-6}$	0.2421	0.7541
0.1778			0.9999	$1.165 \cdot 10^{-4}$	$9.176 \cdot 10^{-2}$	0.9037
0.2371			0.9996	$3.684 \cdot 10^{-4}$	$3.097 \cdot 10^{-2}$	0.9642
0.3162			0.9986	$1.164 \cdot 10^{-3}$	$1.001 \cdot 10^{-2}$	0.9851
0.4217			0.9956	$3.669 \cdot 10^{-3}$	$3.197 \cdot 10^{-3}$	0.9919
0.5623			0.9862	$1.149 \cdot 10^{-2}$	$1.021 \cdot 10^{-3}$	0.9941
0.7499			0.9576	$3.527 \cdot 10^{-2}$	$3.309 \cdot 10^{-4}$	0.9949
1.000	0.9999	$1.321 \cdot 10^{-5}$	0.8773	0.1021	$1.110 \cdot 10^{-4}$	0.9953
1.259	0.9999	$3.306 \cdot 10^{-5}$	0.7405	0.2152	$4.820 \cdot 10^{-5}$	0.9958
1.585	0.9999	$8.400 \cdot 10^{-5}$	0.5336	0.3882	$2.179 \cdot 10^{-5}$	0.9963
1.995	0.9997	$2.110 \cdot 10^{-4}$	0.3167	0.5696	$1.018 \cdot 10^{-5}$	0.9969
2.512	0.9993	$5.296 \cdot 10^{-4}$	0.1612	0.7020	$4.877 \cdot 10^{-6}$	0.9974
3.162	0.9984	$1.329 \cdot 10^{-3}$	$7.684 \cdot 10^{-2}$	0.7791	$2.374 \cdot 10^{-6}$	0.9979
4.217	0.9949	$4.189 \cdot 10^{-3}$	$3.092 \cdot 10^{-2}$	0.8348		
5.623	0.9841	$1.310 \cdot 10^{-2}$	$1.290 \cdot 10^{-2}$	0.8751		
7.499	0.9514	$4.003 \cdot 10^{-2}$	$5.405 \cdot 10^{-3}$	0.9062		
10.00	0.8611	0.1144	$2.270 \cdot 10^{-3}$	0.9295		
13.34	0.6633	0.2775	$9.552 \cdot 10^{-4}$	0.9471		
17.78	0.3875	0.5055	$4.023 \cdot 10^{-4}$	0.9603		
31.62	$6.900 \cdot 10^{-2}$	0.7802	$7.147 \cdot 10^{-5}$	0.9776		
42.17	$2.822 \cdot 10^{-2}$	0.8334				
56.23	$1.193 \cdot 10^{-2}$	0.8742				
74.99	$5.035 \cdot 10^{-3}$	0.9057				
100.0	$2.123 \cdot 10^{-3}$	0.9293				
177.8	$3.775 \cdot 10^{-4}$	0.9602				
316.2	$6.713 \cdot 10^{-5}$	0.9776				

If we define $C_r/C_{r0} = (C_P - C_\infty)/(C_0 - C_\infty)$ and $G_r/G_{r\infty} = G_P/G_\infty (\mu' = \infty)$, it is found that these quantities depend on frequency very similarly to those shown in Fig. 1 for motional dispersion and, like them, agree with Debye curves over a considerable frequency range. Thus, the equivalent series values of recombination capacitance/cm² and conductance/cm² will be $C_{r0} = (C_0 - C_\infty)$ and $G_{r\infty}$. These values may be determined from

$$\frac{C_\infty}{C_0} = \frac{(M/\sqrt{2}) \coth(M/\sqrt{2}) - 1}{M \coth M - 1}, \quad (75)$$

and

$$G_{r\infty}/G_\infty = \left[(M/\sqrt{2}) \coth(M/\sqrt{2}) - M^2 \{4 \sinh^2(M/\sqrt{2})\}^{-1} \right] \xi^{-1}. \quad (76)$$

Like the motional case, the actual series value of capacitance drops from $(C_0 - C_\infty)$ toward zero for very high frequencies. Similarly, the series conductance drops to a limiting value less than $G_{r\infty}$ at low frequencies. Nevertheless, unless M is very small, the series values may be considered frequency-independent over the frequency range of experimental interest. As in

TABLE IV. The dependence of the value of $\sqrt{\nu_m}$ at $C_P/C_0 = G_P/G_\infty$ on M and ξ . The Debye value is unity.

$\xi \setminus M$	10^{-1}	1	10	20	100	10^4
0	0.9598	0.9612	0.9888	0.9938	0.9990	0.9999
100	1.138	1.130	1.056	1.055	0.9821	0.9999

$M \setminus \xi$	0	10	10^2	10^4	10^6	10^8
10	0.9888	0.9681	1.0692	1.0857	1.0860	1.0860

the motional dispersion case, we may now define a macroscopic recombination time constant τ_R , given by

$$\tau_R = \left[\frac{\coth M - (1/\sqrt{2}) \coth(M/\sqrt{2})}{(1/2\sqrt{2}) \coth(M/\sqrt{2}) - M \{4 \sinh^2(M/\sqrt{2})\}^{-1}} \right] \tau_r. \quad (77)$$

Except for the term in the brackets, which approaches $2(\sqrt{2}-1)$ as M increases, τ_R is thus equal to τ_r .

The foregoing results may now be utilized to construct an equivalent circuit for unit area of the layer of thickness L which consists, within the limitations discussed above, of frequency-independent elements. The circuit will apply for any value of ξ and will be valid over a wider frequency range the larger the value of M . The circuit is given in Fig. 5. It is easily verified that this configuration gives the correct frequency response. For example, when ξ/M is much less than unity, Eq. (79) shows that $G_{r\infty}/G_\infty$ will be very large. The conductance/cm² $G_{r\infty}$ may then be neglected, and the space-charge branch of the circuit reduces to C_0 and G_∞ in series as previously found for the case $\xi=0$. Similarly, for $\xi=\infty$ (complete dissociation), $G_{r\infty}$ is zero, and the series arm consists of C_∞ and G_∞ . When it is remembered that G_∞ is just the ordinary ohmic con-

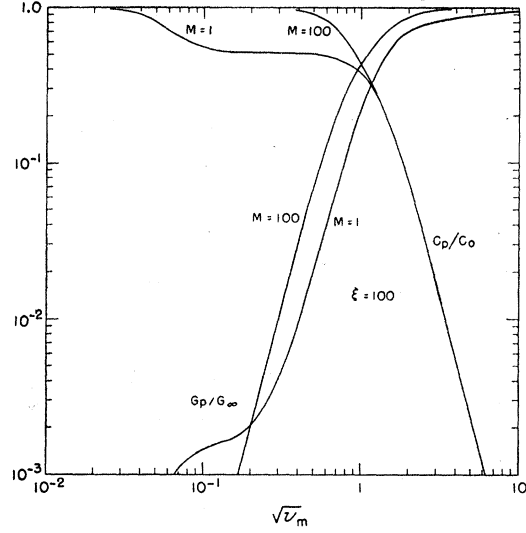


FIG. 2. Doubly logarithmic plot of C_P/C_0 and G_P/G_∞ versus $\sqrt{\nu_m}$ for $\xi=100$ and $M=1$ and 100 .

ductance/cm² of the layer in the absence of blocking at either electrode, it is easily seen from Fig. 5 that the effect of blocking is to introduce the additional elements shown. If only one electrode is blocking, the equivalent circuit of a layer $L/2$ thick with one electrode blocking, one nonblocking will be exactly like that shown in Fig. 5, but with all elements doubled. This result is readily verified from a consideration of the symmetry about the plane at $L/2$ of a slab of thickness L with both electrodes blocking. Since carriers pass freely across the center plane and the two halves are exactly alike and essentially in series, the capacitance and conductance of either half with one blocking and one nonblocking electrode must be twice that of both together.

IV. COMPARISON WITH EXPERIMENT AND WITH OTHER THEORIES

In this section we shall consider how the theoretical results can be best compared with experiment to obtain

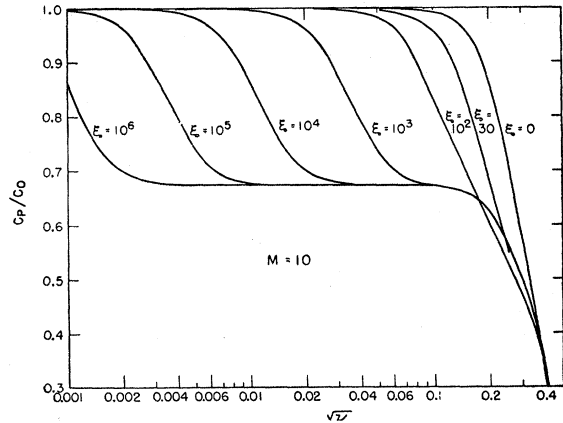


FIG. 3. Semilogarithmic plot of C_P/C_0 versus $\sqrt{\nu}$ for $M=10$ and various ξ values.

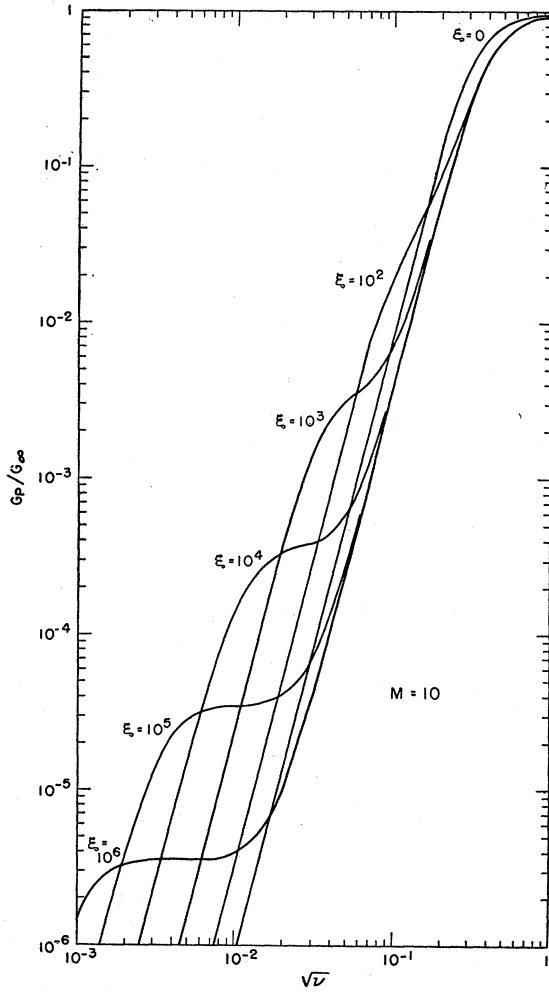


FIG. 4. Doubly logarithmic plot of G_P/G_∞ versus $\sqrt{\nu}$ for $M=10$ and various ξ values.

c_0 , μ' , and ξ , and how the present theory compares with some other theories of space-charge effects. It is obvious from the preceding work that c_0 , μ' , and ξ can be calculated if C_g , C_0 , G_∞ , C_∞ , and G_{r_∞} can be obtained from the experimental results.²⁰ Not all these quantities are necessary, of course, but some are easier to work with than others. First, if measurements can be extended to sufficiently high frequencies, the measured parallel capacitance/cm² and conductance/cm² will approach C_g and G_∞ . In the experimental situation where charge carriers are mobilized by absorption of light, C_g can be determined at any convenient frequency by measurement in the dark. Alternatively, it can be calculated if the dimensions and dielectric constant of the sample are known. Assuming that C_g is known and that measured values of parallel capacitance/cm² and conductance/cm² are available over the frequency range of interest, one then may subtract C_g from the measured values to

²⁰ It is possible to calculate only D' and not μ' unless the Einstein relation is employed.

obtain C_P at each frequency. The measured conductance/cm² will be G_P in the absence of other loss and conduction mechanisms. If the shapes of the G_P and C_P curves versus frequency approximate well to Debye curves with the same relaxation time, it may be concluded that recombination is rapid and ξ/M is less than about 0.1, or alternatively, that both positive and negative carriers are mobile with equal mobilities, or finally, that they have different mobilities but very rapid recombination. The correspondence of the experimental curves to Debye curves may be tested either by conversion of the parallel values to equivalent series values or in the following way. If G_P depends on frequency according to a Debye curve, the quantity $G_P/(G_\infty - G_P)$ plotted versus ω^2 should give a straight line of slope τ_m^2 . Likewise $(C_0/C_P - 1)$ versus ω^2 should also yield a straight line of slope τ_m^2 . The τ_m values obtained from these two lines should be the same, provided the C_P and G_P curves involve the same dispersion mechanism. Further, the value of τ_m obtained from crossover ($C_P = G_P/\omega_1$) should also be the same as that obtained from the straight-line plots.

When the curves approximate well to Debye curves over a wide frequency range, the quantity ξ cannot be obtained from simple frequency dependence measurements. However, μ' and C_0 may be calculated from either the curve of C_P versus frequency or that of G_P versus frequency. This is a valuable result since it often may happen that measurements cannot be extended to a sufficiently low or a sufficiently high frequency to yield both C_0 and G_∞ . If one or the other of these quantities can be determined together with τ_m , Eq. (75) shows that the other may be immediately computed. Of course, the experimental determination of C_0 , G_∞ , and τ_m furnishes an additional check on the correctness of all of these values.

TABLE V. Dependence of recombination dispersion values of C_P/C_0 and G_P/G_∞ on $\sqrt{\nu_r}$. The values of G_P/G_∞ for $M=10^2$ are identical with those for $M=10$.

$\sqrt{\nu_r}$	$M=1$		$M=10$		$M=10^2$
	C_P/C_0	G_P/G_∞	C_P/C_0	G_P/G_∞	C_P/C_0
0.1000	1	$9.421 \cdot 10^{-5}$	1	$7.071 \cdot 10^{-5}$	1
0.1334	0.9999	$2.979 \cdot 10^{-4}$	0.9999	$2.236 \cdot 10^{-4}$	0.9999
0.1778	0.9995	$9.412 \cdot 10^{-4}$	0.9998	$7.066 \cdot 10^{-4}$	0.9998
0.2371	0.9986	$2.970 \cdot 10^{-3}$	0.9992	$2.231 \cdot 10^{-3}$	0.9993
0.3162	0.9955	$9.333 \cdot 10^{-3}$	0.9976	$7.016 \cdot 10^{-3}$	0.9978
0.4217	0.9860	$2.893 \cdot 10^{-2}$	0.9925	$2.182 \cdot 10^{-2}$	0.9932
0.5623	0.9583	$8.609 \cdot 10^{-2}$	0.9775	$6.561 \cdot 10^{-2}$	0.9796
0.7499	0.8888	0.2294	0.9387	0.1798	0.9442
1.000	0.7650	0.4850	0.8461	0.4028	0.8764
1.259	0.6594	0.7026	0.7927	0.6218	0.8115
1.585	0.5853	0.8557	0.7359	0.8007	0.7599
1.995	0.5459	0.9371	0.7025	0.9084	0.7295
2.512	0.5281	0.9740	0.6864	0.9610	0.7149
3.162	0.5206	0.9894	0.6794	0.9841	0.7085
4.217	0.5171	0.9966	0.6761	0.9949	0.7056
5.623	0.5160	0.9989	0.6751	0.9984	0.7046
7.499	0.5156	0.9995	0.6747	0.9995	0.7043
10.00	0.5155	0.9998	0.6746	0.9998	0.7042
17.78	0.5155	1	0.6746	1	0.7042
31.62	0.5155	1	0.6746	1	0.7041

When the curves of G_P and C_P versus frequency show well-defined double dispersion, the quantity ξ (and so k_2 and k_1) may be determined in addition to μ' and C_0 , provided it can be established that the lower-frequency dispersion region is in fact due to recombination. ξ can then be determined either from the G_P curve using Eq. (79) or from the C_P curve by subtracting out the motional capacitance/cm², C_∞ , and determining τ_r from the remaining recombination dispersion curve. In the intermediate region where the curves are rounded by recombination but no plateaus appear, ξ can only be determined from a detailed comparison of theoretical and experimental curve shapes for different values of ξ . A qualitative comparison of the present theory and some experimental results on electrolytes, semiconductors, and photoconductors has already been given.¹⁹ A quantitative comparison with experimental data on the photocapacitive effect⁴ will be published later.

It is worth noting that the Fuoss-Kirkwood many relaxation time theory⁵ cannot be used to accurately fit the dispersion curves when ξ is greater than zero except in the trivial case for which ξ is sufficiently small that the dispersion curves are well approximated by Debye curves with a single relaxation time. The reason for this failure is, of course, that as ξ increases from zero, two relaxation times appear in our theory, and these times are not in general equal. On the other hand, the Fuoss-Kirkwood theory postulates a distribution of relaxation times spread about a most probable time. Even in the case $\xi=0$ and $M < 1$, for which the deviations from Debye curves are fairly considerable, the Fuoss-Kirkwood theory will not allow a good fit of the dispersion curves to be obtained. Again, this is not an unexpected result.

Next, it is of interest to compare the results of the present theory with those of other space-charge theories. The present theory predicts the possibility of two dispersion regions, one at low frequencies arising from finite recombination time and the other, at higher frequencies, produced by the finite mobility of charge carriers. Recombination cannot relax the space-charge capacitance by more than a factor of $\sqrt{2}$ unless M is small, and motional relaxation does not reduce the total capacitance by more than a factor of about M .

Lawson, Miller, Schiff, and Stephens^{21,22} have developed a theory to account for the dispersion of the parallel capacitance and conductance of the barrier layer of a crystal rectifier based on a dispersion mechanism not explicitly considered in the present work. In the frequency range to which this mechanism is to apply, these authors assume that the recombination time is short compared to a half cycle and that the mobility is sufficiently high that free carriers can always

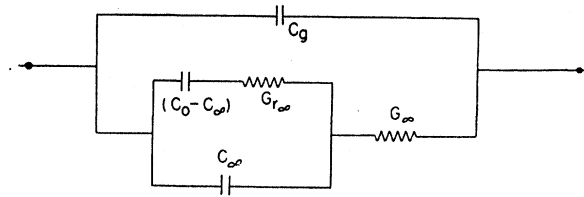


FIG. 5. Equivalent circuit for unit area of a capacitor containing mobile charge carriers of only one sign for which both electrodes are blocking.

stay in phase with the applied voltage. Dispersion then arises from the fact that some carriers will be bound to impurity ions within the barrier layer. When the phase of the applied voltage is such that free carriers leave the barrier layer, the additional carriers bound to impurity ions will be unable to leave immediately but will be delayed by the average ionization time k_1^{-1} . Since k_1 is the probability per unit time for ionization, the delay will be negligible as long as k_1 is much greater than the frequency of the applied voltage, but dispersion will occur when these quantities are comparable. This trapping-time dispersion may occur either above or below the frequencies at which motional dispersion takes place, depending on the magnitudes of the mobility and k_1 . However, if motional dispersion occurs at the lower frequency, it will relax the barrier layer capacitance and no further change will be observed at higher frequencies.

This theory of Lawson *et al.* only applies to rectifiers having barrier layers of the order of 10^{-6} cm thick, to which the diode rectification theory also applies. The neglect of motional effects implies that an electron produced in the barrier layer will leave that layer and reach the bulk material in a time short compared to a half-cycle of the frequency concerned. For thick barriers of the order of 10^{-4} to 10^{-3} cm thick, to which the diffusion rectification theory applies, an electron will be unable to traverse the layer in a half-cycle of the frequency at which trapping-time dispersion takes place. This frequency is of the order of 10^9 to 10^{10} cps in most crystal rectifiers. Thus, in this latter case, motional dispersion would occur at lower frequencies than the above. Experimentally, the dispersion in rectifiers having thick barrier layers does indeed occur at frequencies several orders of magnitude below 10^{10} cps and the present discussion therefore indicates that all or part of such dispersion may be a motional effect.

Although the present theory and that of Lawson *et al.* are both space-charge dispersion theories, the fact that the dispersions arise from different causes makes any direct comparison between them relatively useless. However, as an aid to distinguishing between the two in experimental cases, Fig. 6 shows how the respective normalized curves for the two theories differ in their frequency dependence. Both sets of curves apply to the small dissociation case only. The frequency scales have been adjusted to make the capacitance curves coincide

²¹ Lawson, Miller, Schiff, and Stephens, National Defense Research Council Report NDRC-14-153, July 1, 1943 (unpublished).

²² H. C. Torrey and C. A. Whitmer, *Crystal Rectifiers* (McGraw-Hill Book Company, Inc., New York, 1948).

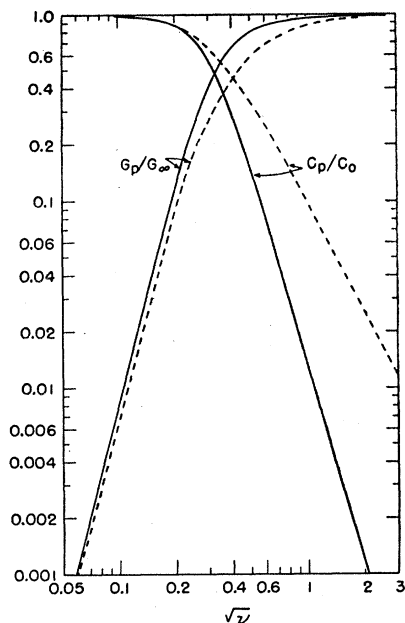


FIG. 6. Comparison of finite-ionization-time dispersion curves (dotted lines) with motional dispersion curves (solid lines) plotted for $M=10$, $\xi=0$ (see references 11 and 12). Frequency scales have been adjusted to make capacitance curves coincide at low frequencies.

at low frequencies. It will be noted that the principal deviations occur in the capacitance curves.

Finally, let us compare the present theory with that of Chang and Jaffé.³ We have already seen that for $M \gg 1$, the values of C_0 and G_∞ obtained from the present theory are in agreement with those of Chang and Jaffé. Even in this case, the frequency dependence of C_P/C_0 and G_P/G_∞ are considerably different, however. Chang and Jaffé derive formulas for the frequency dependence of the capacitance and conductance of the polarization layer $l (\ll L)$ only. To obtain the parallel values for the entire layer L , they would be forced to convert their parallel values to series values, add in the series resistance of the bulk layer of thickness $(L-l)$, and finally convert the resulting series values to parallel values. Since l is also a function of frequency, this is a tedious process and it yields results applicable to only a single value of L each time it is carried out. The Chang-Jaffé results for the polarization layer l alone yield capacitance and conductance curves which differ markedly from our results.

Rather than compare our results with those of Chang and Jaffé for a single value of L , we shall instead compare them with the results of an earlier theory of Chang and Jaffé which are not corrected for frequency variation of the thickness of the polarization layer.³ In this work, instead of assuming an inhomogeneous electric field within the entire layer L , Chang and Jaffé postulated a real constant field and derived the resulting space-charge capacitance and conductance for the entire layer of thickness L on the basis of this

assumption. Since, as we have seen, the actual field is complex and may be essentially zero near the middle of the slab and exceedingly inhomogeneous near the boundaries, this is not a very good assumption. It leads to the correct value of G_∞ but to $C_0 = e\mu c_0 L / 6D$. Thus, the dimensionless frequency variable which Chang and Jaffé use is not the same as either of the variables ν_m or ν used herein. The relative curve shapes are not as greatly different from those of the present theory as one might expect, however. Figure 7 shows the comparison of normalized capacitance and conductance curves for the two theories. Since the Chang-Jaffé theory applies only to positive and negative charge carriers of the same mobility and no recombination, we have made the comparison on the same basis ($\sigma=1$, $M=10$). Here, the frequency scales have again been shifted to make the capacitance curves coincide at low frequencies, and we see that the principal deviations occur between the respective G_P/G_∞ curves. The Chang-Jaffé curves do not, of course, agree well with Debye curves. The present theory is an improvement on the Chang-Jaffé theory in the following ways:

- (a) The theory is intrinsically more accurate since the electric field satisfies Poisson's equation;
- (b) The results apply to the entire layer L and follow Debye curves quite well in their frequency dependence, so that an illuminating equivalent circuit of the layer may be constructed;
- (c) The theory applies for any recombination time and any degree of dissociation;
- (d) The equations of the theory have been solved for any ratio of the mobilities of positive and negative carriers.

In conclusion, we should mention that the theory derived in this paper is not sufficiently general to apply to all space-charge effects of interest. First, the results when positive and negative carriers have different nonzero mobilities have only been given in terms of a complicated formula, not tabulated and graphed. It is hoped to rectify this omission in a later paper devoted mainly to electrolytes. Second, the assumption that all the charge carriers in the material dissociate from the same kind of neutral centers will often be too restrictive. However, although the extension of the equations of detailed balance to include, for example, the presence of extraneous traps for one or more species of charge carrier changes the frequency dependence of η^\pm , it will not in general change the form of the solution of the equations. Thus, the present solution is a good beginning for the analysis of more complicated situations. Such extension has been carried out and will be further discussed in the later paper on the photocapacitative effect.

ACKNOWLEDGMENTS

The author wishes to thank Mr. Elwin L. Dershem for programming the final formulas for the IBM card

programmed computer and for carrying out the calculation of many frequency-dependence tables. In addition, the author is much indebted to the Argonne National Laboratory for a visiting appointment.

GLOSSARY OF PRINCIPAL SYMBOLS

- C_g Geometrical capacitance/cm² of layer. (45)²³
 C_P Space-charge polarization parallel capacitance/cm² of layer. (44, 53)
 C_S Space-charge polarization series capacitance/cm² of layer.
 C_0 Zero-frequency limiting value of C_P for finite recombination time. (55)
 C_∞ Zero-frequency limiting value of C_P for infinite recombination time; also high-frequency limiting value of C_P for finite recombination time, infinite mobility. (75)
 C_r Recombination contribution to C_P . It equals $(C_P - C_\infty)$.
 C_{r0} Zero-frequency limiting value of C_r .
 c_0 Average, static charge density of positive and/or negative charge carriers.
 D Diffusion coefficient of positive charge carriers.
 D' Diffusion coefficient of negative charge carriers.
 $E(x)$ Electric field strength. Static component E_0 ; fundamental frequency component E_1 .
 e Absolute value of electronic charge.
 f Electrical frequency.
 G_P Space-charge polarization parallel conductance/cm² of layer. (44, 54)
 G_S Space-charge polarization series conductance/cm² of layer.
 G_∞ High-frequency limiting value of G_P . (56)
 G_0 Low-frequency limiting value of G_S . (71)
 G_r Recombination contribution to G_P .
 $G_{r\infty}$ High-frequency limiting value of G_r . (76)
 $j_1(x)$ Fundamental frequency component of current density within the layer.
 J_1 Fundamental frequency component of current density entering layer.
 k Boltzmann's constant.
 k_1 Dissociation constant. Probability per unit time for dissociation of neutral centers.
 k_2 Recombination constant. Related to average recombination rate. (24).
 L Thickness of layer between electrodes.
 L_D Root-mean-square Debye length. (57)
 M Dimensionless variable which measures the number of rms Debye lengths contained in L . (31, 57)
 N Initial homogeneous concentration of neutral centers before dissociation.
 n Concentration of negative carriers. Static component n_0 ; fundamental component n_1 .
 n_c Concentration of neutral centers after dissociation. Static component n_{c0} ; fundamental component n_{c1} .
 p Concentration of positive carriers. Static component p_0 ; fundamental component p_1 .
 r Dimensionless variable equal to M for large M and small dissociation. (58)
 T Absolute temperature.
 V Applied voltage; fundamental component V_1 .
 δ Ratio of fundamental component of charge bound in neutral centers to fundamental component of total charge, free and bound. (48)

²³ Numbers in parentheses are those of the most important defining equations for the symbol considered.

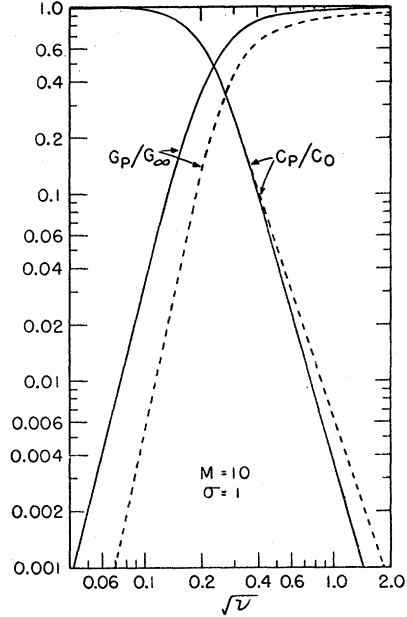


FIG. 7. Comparison of the results of the present theory for $\sigma = 1$, $M = 10$ (solid lines) with those of Chang and Jaffé (dotted lines) who assume a homogeneous electric field. Positive and negative charge carriers of equal mobility, complete dissociation.

- ϵ Ordinary dielectric constant of material in absence of free charges.
 η^\pm Dimensionless quantities involving both the Debye length and frequency. They largely determine the space-charge polarization frequency response. (41)
 η_0^- Zero-frequency value of η^- in the case of negative carriers alone mobile. η_0^- equals M for small dissociation.
 λ Ratio of fundamental component of charge bound in neutral centers to fundamental component of free charge. (23)
 μ Microscopic mobility of positive charge carriers.
 μ' Microscopic mobility of negative charge carriers.
 ν Dimensionless frequency variable. (33)
 ν^* Dimensionless frequency variable equal to $\omega\tau_D$. (46)
 ν_m Macroscopic dimensionless frequency variable equal to $\omega\tau_m$. (74)
 ν_r Dimensionless frequency variable equal to $\omega\tau_r$. (24)
 ξ Ratio of average recombination time to dielectric relaxation time. (47)
 ρ^\pm Complex roots of auxiliary equation which determine frequency and x dependence. (34)
 σ Ratio of mobility of negative carriers to mobility of positive carriers. (32)
 σ_∞ High-frequency limiting value of conductivity of layer.
 τ_D Dielectric relaxation time for conductivity σ_∞ . (46)
 τ_m Motional or capacitive relaxation time associated with the decay of the space-charge layers near the electrodes. (72)
 τ_r Mean lifetime of an excess carrier for recombination. (24)
 τ_R Macroscopic recombination time constant. (77)
 ω Radial frequency.
 ω_1 Radial frequency at which Debye curves cross

$$\omega_1 = G_P(\omega_1)/C_P(\omega_1) \cong \tau_m^{-1}.$$